ISSN 0016-8696 · Gerlands Beitr. Geophysik · Leipzig · 98 (1989) 4 · S. 312–321

The Berhida (Hungary) earthquake of 1985

By **L. Tóth, P. Mónus** and **T. Zsíros,** Budapest*)

With 6 Figures and 3 Tables

Received June 8, 1988, revised paper December 5, 1988

Summary

The earthquake on August 15, 1985, in Berhida in Hungary was widely felt and followed by more than two hundred aftershocks during several months. Isoseismal maps, derived from macroseismic observations and attenuation curves are presented. From the maps a focal depth of $h = 12$ km and a related attenuation factor of -0.0065 can be estimated. The focal mechanism solution shows strike-slip faulting with a nearly horizontal compressional stress axis oriented E–W.

Key words: seismicity, focal mechanism, Pannonian Basin.

Zusammenfassung

Das Erdbeben von Berhida in Ungarn am 15. August 1985 wurde weithin wahrgenommen. Im Verlaufe einiger Monate folgten ihm über 200 Nachbeben. Es wurden hier aus makroseismischen Beobachtungen zusammengestellte isoseismische Karten und Dämpfungskurven vorgestellt. Auf Grund der Karten können eine Herdtiefe von $h = 12$ km und ein entsprechender Dämpfungskoeffizient von $-0{,}0065$ geschätzt werden. Der Herdmechanismus weist eine Transversalverschiebung auf, wobei die Achse der Kompressionsspannung von Ost nach West verläuft.

Резюме

Землетрясение 15 августа 1985 года в Берхиде (Венгрия) далеко замечалось. Ему следовало более 200 афтершоков в течение нескольких месяцев. Представлены изосейсмические карты, составленные на основе макросейсмических данных, а также кривые затухания. Из карт можно делать вывод, что глубина очага = 12 км, а соответствующий коэффициент затухания составляет — 0,0065. Очаговой механизм выявляет поперечный сдвиг с почти горизонтальной осью сжимающей нагрузки с направлением В—З.

Introduction

Hungary represents a region of low seismicity on the average with two-three shallow earthquakes above 2.5 m_b threshold value being recorded annually by the Hungarian Seismograph Station Network, with the exception of seismic sequences

* Dr. L. Tóth, Geodetic and Geophysical Research Institute, Hungarian Academy of Sciences, Meredek u. 18, H-1112 Budapest, Hungary.

as in 1985 or 1956, when the relatively strong event was followed by hundreds of aftershocks. During the last thirty years, the strongest recorded earthquake (Dunaharaszti 1956) had a magnitude of 5.5 m_b (CSOMOR, 1967).

On 15 August, 1985 (04h 28m GMT), an earthquake of magnitude 4.7 m_b (NEIC) occurred in the western part of the Pannonian Basin. So far, it is one of the largest earthquakes that has taken place in the area during this century. The shock caused moderate damage in the Berhida-Peremarton area. Slight damage was reported from Budapest. The quake was felt throughout western Hungary, at Komarno, at Nove Zamky and Hurbanovo and at Bratislava, Czechoslovakia. It was also felt at Zagreb, Yugoslavia and in Burgenland and at Vienna, Austria. The maximum intensity has been estimated VII on the MSK-64 scale.

Earthquakes in the Pannonian Basin are crustal events, sometimes followed by series of aftershocks. The relatively strong earthquake near lake Balaton (Fig. 1), Berhida on August 15, 1985 was preceded by 3 foreshocks and followed by 29 aftershocks with a magnitude greater than 3.0. A large number of smaller aftershocks occurred in the area after the major shocks. At least 226 aftershocks were identified from 15 August, 1985 to 30 July, 1986.

The main shock was well recorded by many stations providing an excellent opportunity to study the focal mechanism.

This paper contains three contributions with different topics on this event. In the first part, macroseismic information is compiled in maps, and derived attenuation curves are presented. Further on, the historical seismicity, regional geology and tectonics are examined. Finally, the fault plane solution and the relationship of the source mechanism and the tectonic situation in the region are discussed.

Macroseismic and instrumental data

The earthquake caused moderate and some heavy damage, deep cracks in walls, fall of chimneys, tombstones overturned etc. in the Peremarton-Berhida epicentre region and at some localities on the shore of Lake Balaton. The maximum intensity has been estimated VII on the MSK scale.

The macroseismic data were collected from 275 localities in Hungary, and the distribution of felt intensities is shown in Fig. 1.

The isoseismal map strikingly reflects the different propagation of seismic energy in NW and SW directions (Figure 2).

The focal depth (h) and the absorption coefficient (α) were estimated by the Kövesligethy formula using the mean radii $R(I = 5.5) = 23$ km, $R(I = 5) = 53$ km, $R(I = 4) = 112$ km. The results are $h = 12.4$ km and $\alpha = -0.0065$ with a standard deviation of 2.5 and 0.0051, respectively.

The negative value of the absorption coefficient naturally is not conform with the physical idea in the case of energy. But in Kövesligethy's formula α is defined as coefficient of attenuation of macroseismic effects of earthquakes and from this aspect the negative value of α reflects the reality in some cases. PROCHÁZKOVA (1982) made an effort to solve this virtual contradiction on the basis of holding the assumption of linear relation between $\log E$ (where E is seismic energy) and macroseismic intensity (I). In our understanding we would rather question this explicit relation as macro-

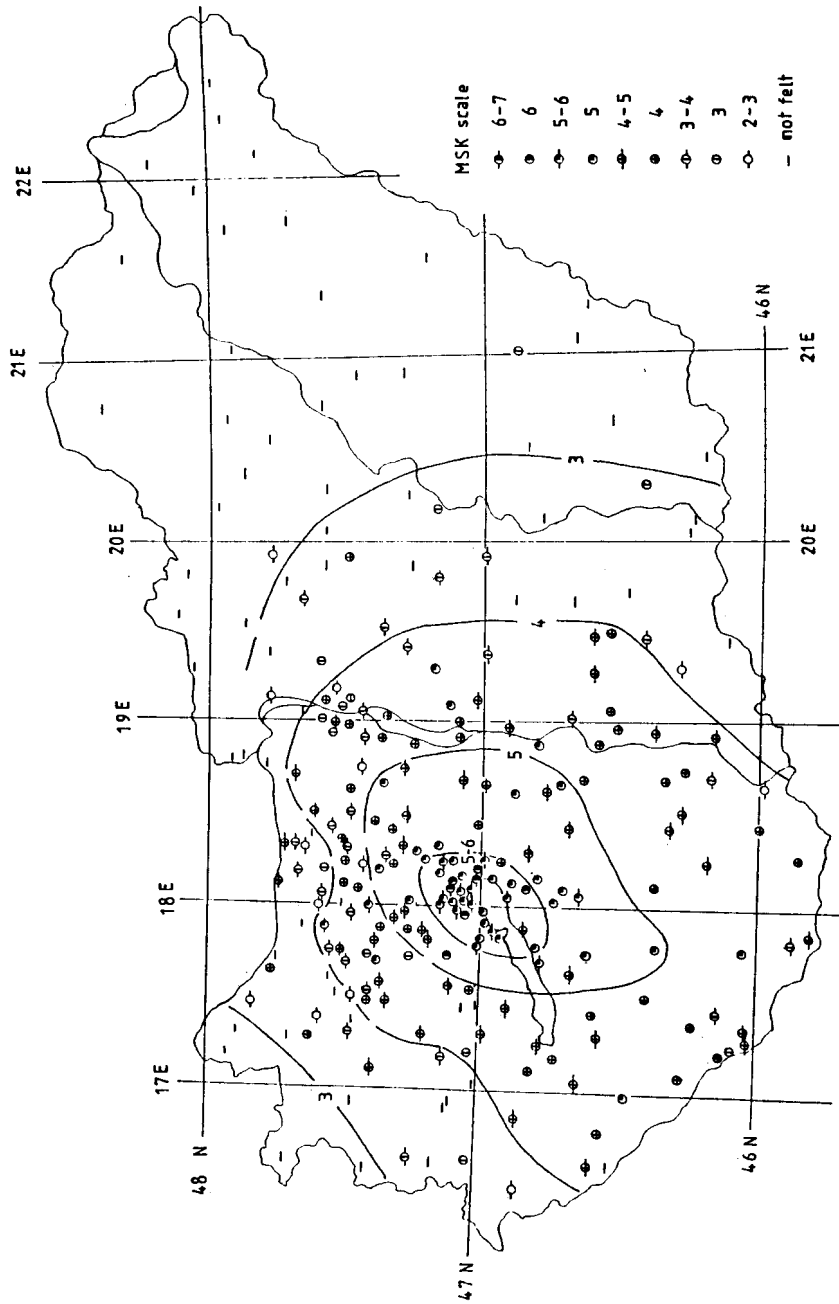

Fig. 1. Distribution of felt intensities and isoseismals in Hungary for the Berhida earthquake of 15 August, 1985

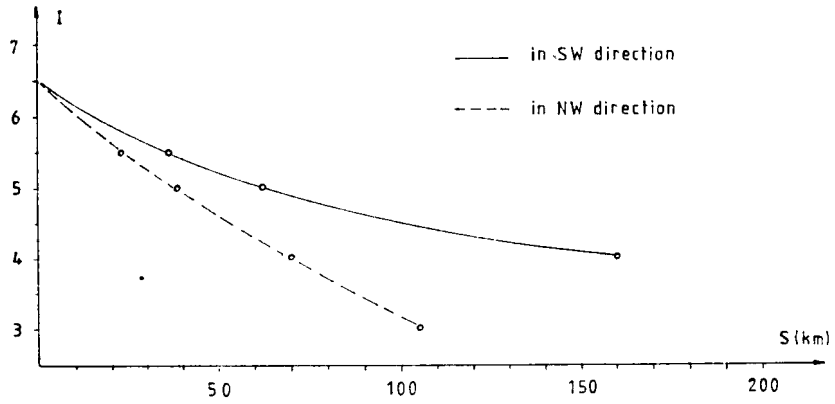

Fig. 2. Intensity attenuation in two different (SW and NW) directions

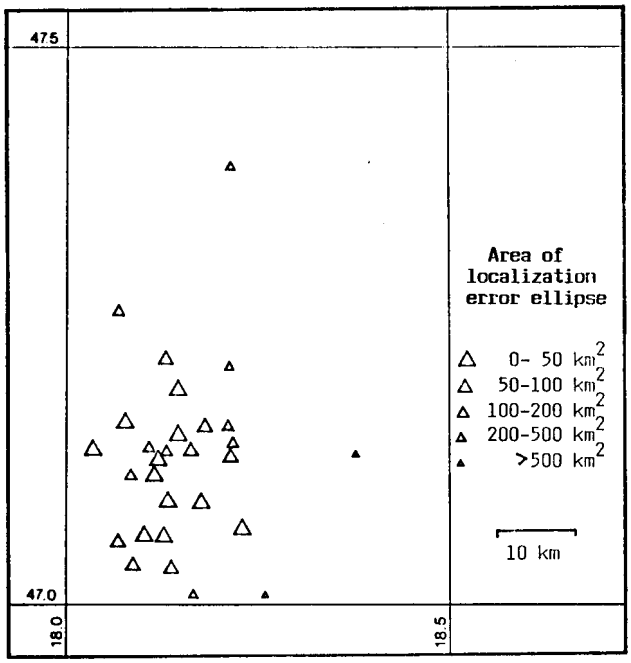

Fig. 3. The epicentre locations and distribution of the 29 greatest aftershocks

seismic effects strongly depend on the spectral distribution of energy and not only on the total energy itself.

The epicentre location and origin time for the main shock and major aftershocks (Figure 3) were computed from arrival times at Hungarian stations. Data from neighbouring countries, from Czechoslovakia, Yugoslavia and Austria were also used. The calculation yielded a focal depth of 12 km for the main shock which is in excellent agreement with macroseismic observations.

Historical seismicity, regional geology and tectonics

Berhida lies just in the Komárom-Balatonkenese line wich is well-known for its relatively high seismicity (Fig. 4).

The largest earthquake that occurred on this seismic line is the Komárom earthquake of June 28, 1763, with an MSK intensity of IX. The second largest event was the January 14, 1810, Mór earthquake with an MSK intensity of VIII. It was quite near to Berhida, the distance is only 30 km.

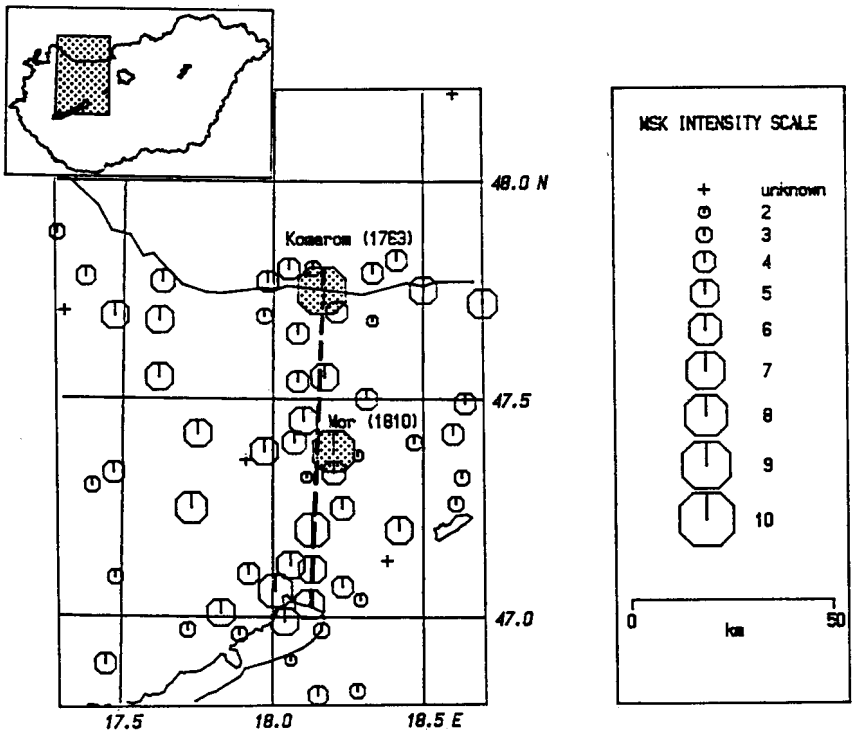

Fig. 4. Historical seismicity in the region of Berhida. Prior to the 1985 earthquake sequence some 700 earthquakes were felt along the Komarom-Balatonkenese line (dotted line) since 1599. The epicentres of the largest events are displayed in the figure

Prior to the 1985 Berhida earthquake sequence, some 700 earthquakes were felt along this line since 1599. The epicentres of the largest ones are shown in Fig. 4.

The Berhida region lies in the north-west continuation of the Balaton Basin. The oldest formation that can be found on the surface is on the NW part of the territory. The Mesozoic basement rock reaches the surface in tracts with a strike of NE—SW direction in this region. This formation consists of mostly Triassic dolomite and limestone.

Most of the region is covered by Quaternary sediments. This is partly Pleistocene river sandy gravel, partly aeolian soil.

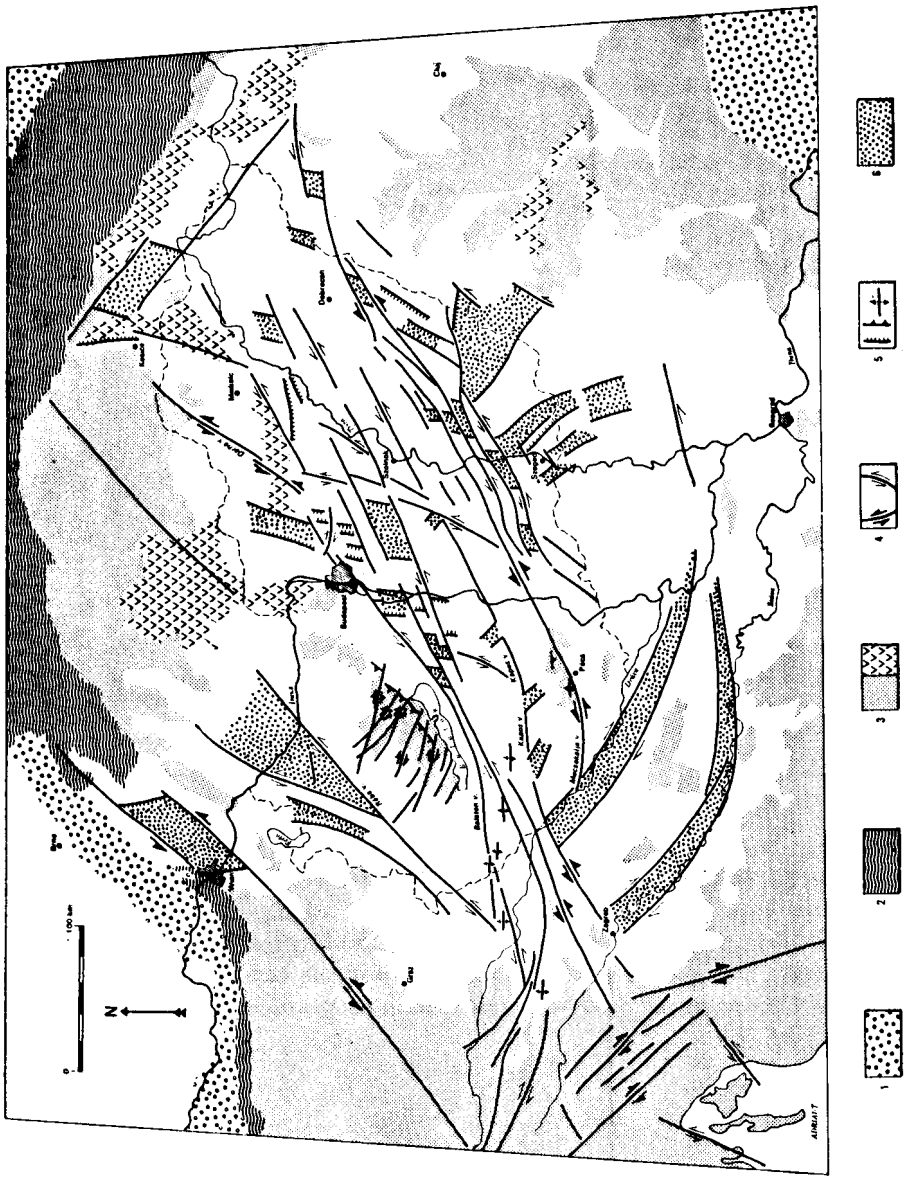

Fig. 5. Tectonic map of the Pannonian Basin and surrounding regions showing the main faults and folds of Neogene age. Tectonic activity culminated during the middle Miocene and has considerably decreased since then. Legend: (1) Molasse foredeep, (2) Alpine Carpathian flysch belt, (3a) Inner Alpine-Carpathian Mountain belt and the Dinarides, (3b) Outcrops of Neogene calcalkaline volcanic rocks, (4) strike-slip faults, the sense (and usually the amount) of displacement is well constrained (thick arrows) or unconstrained (thin arrows), (5) Normal fault, thrust fault and fold, (6) Areas of major crustal extension and subsidence. Figure from Rumpler & Horváth (1988)

Table 1. Epicentre location and origin time for the main shock and major aftershocks

	Origin Time	Lat. (*N*)	Long. (*E*)	Area of localisation error ellipse (km²)
15 August 1985	4 h 13 m 16.1 s	47.26	18.07	173
	4 h 16 m 9.5 s	47.22	18.18	81
	4 h 18 m 25.2 s	47.38	18.21	291
	4 h 28 m 47.1 s	47.06	18.11	50
	4 h 42 m 34.8 s	47.22	18.21	205
	4 h 44 m 33.5 s	47.12	18.12	48
	4 h 51 m 41.1 s	47.01	18.26	532
	5 h 29 m 20.5 s	47.13	18.13	190
	6 h 12 m 40.2 s	47.12	18.09	148
	8 h 58 m 58.1 s	47.14	18.14	59
	9 h 4 m 19.4 s	47.13	18.38	570
	9 h 5 m 33.7 s	47.14	18.11	157
	9 h 54 m 6.7 s	47.06	18.13	13
	10 h 53 m 18.5 s	47.16	18.08	24
	21 h 10 m 20.8 s	47.13	18.13	42
	22 h 57 m 51.1 s	47.01	18.17	253
16 August 1985	0 h 45 m 3.2 s	47.14	18.22	127
	17 h 12 m 59.9 s	47.13	18.22	64
	17 h 25 m 1.4 s	47.19	18.15	32
	20 h 50 m 30.4 s	47.15	18.15	18
17 August 1985	8 h 44 m 1.9 s	47.03	18.14	55
18 August 1985	12 h 28 m 35.4 s	47.03	18.09	85
	16 h 26 m 17.8 s	47.06	18.07	77
19 August 1985	6 h 16 m 29.1 s	47.14	18.04	14
	11 h 14 m 31.8 s	47.09	18.14	15
21 August 1985	16 h 33 m 57.5 s	47.07	18.23	48
29 August 1985	12 h 36 m 59.2 s	47.16	18.18	72
4 Sept. 1985	10 h 04 m 16.4 s	47.16	18.22	152
10 Sept. 1985	0 h 38 m 37.4 s	47.09	18.18	28

The pre-Cainozoic basement has a tract structure in the Berhida region. These tracts have a strike of NE—SW direction with congestion zones on their sides. There is such a striding zone just below Berhida with a NE—SE trend.

The structures of both the Berhida region and the surrounding territory are disrupted by faults. On aerial photographs and on satellite photos one can clearly see that a striding zone trends NE, and also a number of faults with perpendicular strikes (Fig. 5) does so.

Fault plane solution

The conventions for the various parameters used to describe the fault geometry and focal sphere are the same as defined by Aki and Richards (1980). The strike direction is measured clockwise round from north, with the fault dipping down to the right of the strike direction. The dip direction, is measured down from the horizontal perpendicularly to the strike. Slip vector u is taken as the direction of the hanging

Table 2. List of stations used in the focal mechanism determination

station code	azimuth	distance (in deg)	direction of first arrival	station code	azimuth	distance (in deg)	direction of first arrival
SOP	302	1.2	C	STU	289	6.2	C
VKA	317	1.7	C	LLS	271	6.2	D
ZAG	230	1.9	D	PVL	125	6.4	D
JOS	48	2.2	D	SLE	280	6.5	D
LJU	249	2.6	D	VAY	149	6.6	C
MOA	289	2.7	C	ZUL	277	6.6	D
CEY	244	2.8	D	KBN	162	6.7	C
VOY	252	3.1	D	BUH	287	6.8	D
KRA	22	3.2	D	MMB	141	6.8	D
KBA	272	3.2	D	KRL	290	6.8	D
SAR	175	3.2	C	PLD	134	6.9	D
TRI	247	3.3	D	FEL	280	6.9	D
DEV	108	3.5	C	MMK	266	7.0	D
KHC	306	3.6	C	TNS	300	7.1	C
BHG	283	3.6	D	LSK	164	7.1	C
PRU	323	3.7	C	GWF	289	7.3	D
KSP	343	3.9	C	CFR	101	7.3	D
WET	303	4.1	C	DIM	130	7.4	D
BRY	175	4.2	C	DIX	266	7.4	D
NKY	171	4.3	C	KDZ	133	7.5	D
HCY	176	4.6	C	ROF	279	7.6	D
BRG	326	4.7	D	BGG	298	7.8	D
TTG	169	4.7	C	PSN	112	7.9	D
GAP	277	4.8	C	BNS	303	8.2	C
OGA	270	4.8	D	STB	300	8.2	C
BCI	162	4.9	C	GSH	300	8.5	C
CMP	108	5.1	D	MEM	299	8.7	D
SDA	168	5.1	C	ENN	299	8.8	C
HOF	311	5.2	C	COP	340	9.3	C
KKS	161	5.3	C	EZN	137	9.4	D
CLL	324	5.4	D	DOU	294	9.4	C
OSS	269	5.4	D	DST	130	10.7	D
MOX	312	5.6	C	APO	351	13.7	C
SKO	153	5.6	C	LGR	260	15.3	C
PHP	162	5.6	D	ETA	299	16.6	D
VTS	139	5.8	C	JER	133	20.1	D
TIR	167	5.8	D	MOI	133	20.2	D
DUI	207	5.9	C	EVAL	252	20.6	C
VDL	268	5.9	D	LIS	257	21.5	D
SAX	275	5.9	D	BNG	179	42.5	D
BDI	243	6.0	D	BCAO	179	42.5	D
VRI	98	6.1	D	BUL	169	67.5	D
SDI	211	6.2	C	RLO	310	77.8	C
ISR	105	6.2	C	TUL	311	78.4	C

wall, relative to the foot wall. The rake is the angle between strike direction and slip.

The first motion of the *P*-wave displacement was studied on the focal sphere, and a stereographic projection of the lower hemisphere is displayed. *P*-wave first motions shown in Table 2 consist of readings from local, regional and teleseismic distances.

Table 3. Local crustal model in calculation of angle of emergency

h (km)	v_P (km/s)	v_S (km/s)
0—18	5.6	3.2
18—26	7.1	4.1
> 26	8.0	4.6

A lot of the data was read by the authors, and other data were derived from bulletins. For stations at an epicentral distance of more than 20° no ambiguity exists for the angle of emergency from the focal sphere. However, for epicentral distances of less than about 20° multipathing in the upper mantle can complicate the calculation of the appropriate emergent angle. *P*-wave first motions in the epicentral distance range from 2° to 10° were considered to be *Pn* phases. For the calculations the focal depth was fixed at 12 km.

We had used a simple three-layer crustal model to interpret the propagation path for *Pg* and *Pn* phases observed at local and regional distances (Table 3). Using the GUINN and LONG (1977) algorithm to determine all possible regions of *P*, *T* and *B* axes, the same mechanism was obtained.

The focal mechanism solution shows strike-slip faulting with a nearly horizontal compressional stress axis oriented E—W. Nodal planes with strikes 227° and 136° and with respective dips 77° and 76°, as displayed in Fig. 6, fit the observation data.

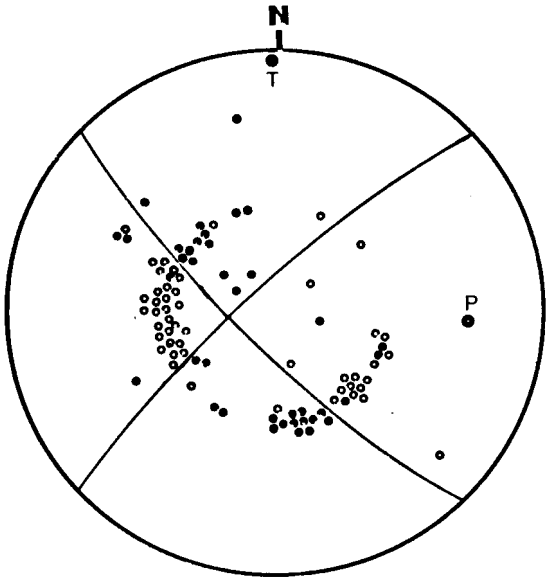

Fig. 6. *P*-wave first motions at 88 different stations for the Berhida earthquake of 1985. Solid circles indicate compression and open circles dilatation. The focal mechanism solution shows strike-slip faulting with a nearly horizontal compressional stress axis oriented in E-W direction. A lower hemisphere stereographic projection of the focal sphere is displayed

Due to the facts that strikes agree with the two general trends of tectonic lines in the area, and that the depth of focus is as great as 12 km, we are not able to discriminate between the nodal planes on the basis of surface geology. The plane with a strike of 227° shows an oblique-normal fault with a slip angle of −166°, close to a pure dextral strike-slip fault. The second nodal plane with its strike of 136° also gives oblique-normal faulting with a slip angle of −13°. This is nearly a pure sinistral strike-slip fault.

Only very limited information on a stress field for the Carpathian Basin is available. The studies of recent tectonics of the area (Horvath, 1984, Grünthal and Stromeyer, 1986) suppose dominant compressive stresses directed N—S. However, the focal mechanism solution presented here resulted in a stress axis oriented E—W.

References

Aki, K., and P. G. Richards 1980: Quantitative Seismology. Theory and Methods, Volume I, pp. 105—115. San Francisco: W. H. Freeman and Co. 1980.

Csomor, D., 1967: Determination of Stresses Acting at the Focus of the Hungarian Earthquake of January 12, 1956. Annal. Univ. Sci. Budapest, R. Eötvös nom., 1966, Sect. Geol., 10, 3—8. (in Russian)

Guinn, S., and L. T. Long 1977: A Computer Method for Determination of Valid Focal Mechanisms using P-Wave First Motions. Earthquakes Notes, Vol. 48, No. 4.

Grünthal, G., and D. Stromeyer 1986: Stress Pattern in Central Europe and Adjacent Areas. Gerlands Beitr. Geophysik 95 (1986) 5, pp. 443—452.

Horváth, F., 1984: Neotectonics of the Pannonian Basin and the surrounding mountain belts: Alps, Carpathians and Dinarides. Ann. Geophysicae 2, 147—154.

Procházková, D., 1982: Attenuation of macroseismic effects of earthquakes. Travaux Geophysiques, XXX, pp. 47—93.

Rumpler, J., and F. Horváth 1988: Some Representative Seismic Reflection Lines from the Pannonian Basin and their Structural Interpretation. In: The Pannonian Basin. A Study in Basin Evolution, AAPG Memoir 45, pp. 153—169. The American Association of Petroleum Geologists, Tulsa, Oklahoma.